Research on Engineering Structures & Materials
www.jresm.org
Research Group

Research Article

Fresh and mechanical behavior of highly flowable concrete incorporating eggshell powder as partial cement replacement

Noor Amnani Mohd Sofi [1,a], Mohd Raizamzamani Md Zain [*,1,2,b], Mohd Fadzil Arshad [1,c]

[1]*Faculty of Civil Engineering, Universiti Teknologi MARA, 40450 Shah Alam, Selangor, Malaysia*
[2]*Structural and Construction Materials Engineering Group, Faculty of Civil Engineering, Universiti Teknologi MARA, 40450 Shah Alam, Selangor, Malaysia*

Article Info

Article History:

Received 09 Oct 2025

Accepted 11 May 2026

Keywords:

Highly flowable concrete;
Eggshell powder;
Fresh properties;
Mechanical properties;
Failure mode

Abstract

This study explores the fresh and mechanical properties of Highly Flowable Concrete (HFC), that utilizes eggshell powder (ESP) as a cement substitute. HFC eliminates mechanical vibration during placement, minimizing segregation and honeycombs while improving construction quality. Considering the increased interest in sustainable alternatives, eggshell powder's calcium content makes it a viable substitute for cement. Thus, laboratory tests were conducted on HFC specimens with eggshell powder substitutions ranging from 5% to 20% by cement weight. The mixture's fresh properties were assessed using slump flow, T500, sieve segregation, and L-box tests. Mechanical performance was examined using compressive and split-tensile strength tests, with specimens tested to failure after 7 and 28 days of curing, respectively. The failure mode of the test specimens was also investigated. The experimental results show that all HFC mixtures containing eggshell powder met the EFNARC fresh properties requirements. Increasing percentages of eggshell powder replacement resulted in improved flowability, reduced segregation, and increased early age strength. The optimal replacement level was found to be 15%. This study provides vital insights into the potential of ESP in improving concrete performance while addressing environmental concerns associated with cement production and paving the way for more sustainable practices in concrete construction.

1. Introduction

The construction industry is expanding rapidly worldwide, especially in Malaysia, where concrete is extensively utilized. However, the usage of conventional concrete, primarily composed of Ordinary Portland Cement (OPC), results in substantial construction costs and environmental degradation owing to high CO_2 emissions from the production of cement [1-3]. In order to alleviate these concerns, self-compacting concrete (SCC), also known as highly flowable concrete (HFC) has been developed as an alternative approach. HFC improves flowability, resists segregation and honeycombing, and minimizes the requirement for vibration during installation, which renders it beneficial for complex formworks and congested reinforcement areas [4].

To improve the performance and sustainability of HFC, researchers investigated the utilization of supplementary cementitious materials (SCMs) generated from industrial and agricultural waste. The incorporation of waste materials such as fly ash (FA), wastepaper sludge ash (WPSA), silica fume (SF), palm oil fuel ash (POFA), rice husk ash (RHA), and ground granulated blast slag (GGBS) improves the workability of HFC while lowering the cement content [5-9]. These supplementary

*Corresponding author: raizam@uitm.edu.my
[a]orcid.org/0009-0008-7837-632X; [b]orcid.org/0000-0002-5356-0410; [c]orcid.org/0000-0002-7342-5822;
DOI: http://dx.doi.org/10.17515/resm2026-1219me1009rs

cementitious materials (SCMs) not only reduce the amount needed for OPC, but also boost particle packing, reduce concrete permeability, and enhance concrete durability [7].

In accordance with this sustainable approach, the current study looks into the utilization of green cementitious materials, particularly eggshell powder, as partial substitutes for OPC in HFC. [10] indicated that GGBS can be employed as a partial replacement for naturally mined limestone while improving durability and speed up the concrete setting process. Similarly, because of the high content of calcium oxide (CaO), eggshell powder (ESP), although being an agricultural waste product, has emerged as a promising materials due to its pozzolanic properties and can be utilized as supplementary cementitious materials [5,11]. Eggshell powder (ESP), produced from waste material, could improve the fresh and mechanical properties of concrete while lowering reliance on OPC.

The performance of ESP-modified HFC is equivalent to that of SCC that incorporates various environmentally friendly supplementary cementitious materials such as fly ash, ground granulated blast furnace slag, rice husk ash, palm oil fuel ash, wastepaper sludge ash, and silica fume [5, 6, 8, 10]. Similar enhancements in flow stability, viscosity modification, and mechanical response were observed across these SCM systems, demonstrating that ESP is competitive and has significant promise as a feasible substitute material in ecologically friendly concrete production. Furthermore, when incorporated into HFC, ESP has the potential to boost the fresh and hardened properties, aligning with the aims of sustainable and green construction practices. Incorporating waste materials as cement substitutes not only enhances concrete properties but also aids with the disposal of solid waste.

A significant aspect of the research is assessing the fresh properties of HFCs incorporating ESP. These properties such as T500, slump flow, segregation resistance and L-box were critical indicators of the concrete's fresh performance. The inclusion of ESP as a cement replacement alters the flow and workability of the concrete mixture. Understanding the unique properties of HFC which includes ESP, such as flowability, viscosity, and segregation resistance, is crucial for optimizing its performance and ensuring its appropriateness for construction applications [5,12].

Aside from fresh characteristics, the mechanical performance of HFC with ESP was explored. This includes assessing its compressive and tensile strength at various curing ages, as well as its durability and resistance to cracking. The experimental investigations conducted by [6] and [13] on other waste-based SCMs emphasizes the necessity of such assessments in establishing the practical usability of alternative materials for structural concrete. Extensive testing for mechanical properties can quantify the potential benefits of using ESP as a partial cement replacement, offering useful insights for designing and implementing sustainable and cost-effective concrete structures.

To shed light on the scope of this investigation, this study focuses on the primary rheological and mechanical properties proposed by EFNARC for identifying Highly Flowable Concrete (HFC). These consist of slump flow, T500, passing ability, and segregation resistance, as well as compressive and splitting tensile strength tests, which are considered as significant indicators of hardened performance. The research conducted stands out in the following aspects: (i) it uses an integrated rheological-mechanical framework for assessing eggshell powder (ESP)-modified HFC, providing a comprehensive understanding of material behaviour; (ii) it develops a predictive regression model for splitting tensile strength based on experimental data; and (iii) it determines optimal ESP replacement levels that provide a balance between workability and mechanical performance. Thus, the findings of this research could have significant implications for the construction industry, particularly in terms of cost reduction and sustainable practices. Through utilizing waste materials such as eggshells, the research aims to promote resource efficiency and waste management while improving concrete performance. This approach promotes resource efficiency and cost savings, aligning with global initiatives to decarbonize the construction industry.

2. Methods

The laboratory study focused on the fresh properties of highly flowable concrete (HFC) with various constituent ingredients. The slump-flow test, carried out in line with [14] was used to

assess the flow characteristics and setting behaviour of HFC. The passing ability was assessed utilizing the L-Box test in accordance with [15], whereas segregation resistance was measured using [16]. Compressive strength testing for the hardened state was conducted on 100 × 100 mm cube specimens following BS EN 12390-1:2012 and BS EN 12390-3:2012. Splitting tensile strength tests were performed on 50 × 100 mm cylindrical specimens with a length-to-diameter ratio of 2.0, using the procedure outlined in BS EN 12390-6: 2009. These mechanical tests were carried out at curing ages of 7, 28, and 90 days to evaluate the short- and long-term strength development of HFC, as discussed in the subsequent topics.

2.1. Materials and Mixture Proportions

The materials that were employed consisted Ordinary Portland Cement (OPC) conforming to Malaysian Standard MS 522, water, natural fine aggregate (≤5 mm), natural coarse aggregate (5–10 mm), eggshell powder (ESP) from discarded eggshells, and SP Master Glenium 8784 superplasticizer, as shown in Fig. 1. ESP was collected from a variety of sources, including local street suppliers, food processing industries, and cafeterias. The obtained eggshells were properly cleansed with tap water to eliminate any organic membranes or contaminants. The eggshell samples were oven-dried at 105 ± 5 °C for 24 hours to remove moisture content. After drying, the eggshells were manually crushed and then ground with a mechanical grinder to produce a fine powder. The ground material was sieved to ensure homogeneous particle size distribution for cement replacement applications. The resulting eggshell powder (ESP) has a fineness similar to cement, indicating its viability as a micro-filler material. It was ground and sieve to a fine powder (Fig. 2) and utilize as a partial cement replacement at 0%, 5%, 10%, 15%, and 20% by weight. The chemical compositions of OPC and ESP, evaluated via X-ray fluorescence (XRF), are displayed in Table 1.

(a) (b) (c) (d) (e)

Fig. 1. HFC constituent materials: (a) cement, (b) grinded ESP, (c) fine aggregates (sand), (d) coarse aggregates, and (e) superplasticizer (Master Glenium 8784)

Fig. 2. Mechanical grinder used for processing eggshells into fine powder (ESP)

It is essential to note that the ESP used in this study was not subjected to calcination. The raw eggshells maintained their original calcium carbonate ($CaCO_3$) form during processing, and the CaO value reported in the XRF results represents the oxide-equivalent convention of XRF analysis, not

actual decomposition. Thus, the value "CaO = 98.8%" in Table 1 corresponds to calcium carbonate content reported as CaO equivalents. A footnote was added to Table 1 to clarify this convention. The current experimental investigations sought to assess the beneficial effects of non-calcined ESP as a sustainable micro filler in HFC. Furthermore, calcination produces free CaO, which can cause volumetric instability and increase the possibility of expansion-related microcracking. $CaCO_3$-based ESP provides stable workability and controlled hydration behaviour, both important in HFC systems. In addition, eliminating high-temperature processing improves economic feasibility, industrial scalability, and carbon efficiency, which aligns with the study's sustainability aims.

Table 1. Chemical composition of ESP and OPC (% by weight)

Compound	ESP (%)	OPC (%)
MgO	< LOD	2.021
Al_2O_3	< LOD	3.7462
SiO_2	< LOD	21.8349
P_2O_5	0.7387	< LOD
SO_3	< LOD	3.5414
K_2O	< LOD	0.2467
CaO	98.8053	64.4872
TiO_2	0.0196	0.197
MnO	< LOD	0.0787
Fe_2O_3	< LOD	3.8159

**Note: LOD denotes the limit of detection CaO represents the oxide-equivalent convention of XRF analysis*

Meanwhile, tap water was utilized as the mixing medium, with a superplasticizer added to improve workability. Fine aggregate filled voids, whereas coarse aggregate ensured structural stability. The standard sieve analysis method was employed for assessing the particle size distribution (PSD) of aggregates, that involved measuring the amount of material retained on a series of sieves with varied apertures. The proportion retained on each sieve was then determined, and the cumulative distribution was plotted resulting in PSD curves for FA and CA, as shown in Figure 3. The findings revealed that the fine aggregates had a well-graded distribution within the standard limits, while the coarse aggregates had a relatively consistent grading pattern, indicating their appropriateness for use in SCC mixtures.

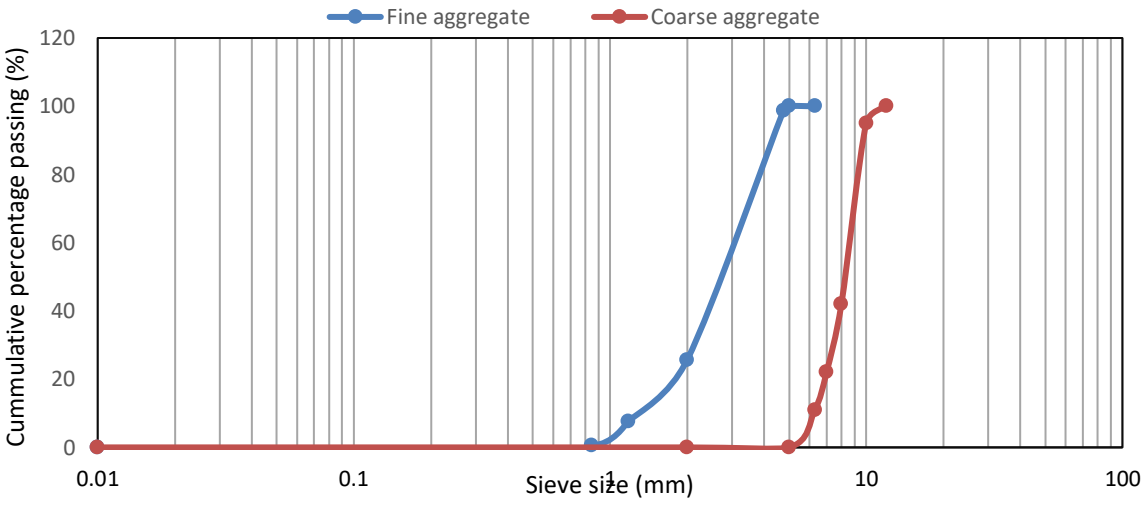

Fig. 3. Particle size distribution of fine and coarse aggregates

The mixtures were blended together to determine the effect of eggshell powder (ESP) on the fresh and mechanical performance of highly flowable concrete (HFC), as well as its suitability as a sustainable construction material. The mix proportions are indicated in Table 2. Thirty specimens had been produced for testing to determine the desired fresh and hardened properties.

The process of mixing highly flowable concrete (HFC) with eggshell powder (ESP) as a partial substitute for Ordinary Portland Cement (OPC) started with the adding of fine and coarse aggregates to the mixing container (Fig. 4a). ESP and OPC were then carefully inserted and mixed with the aggregates to achieve a balanced distribution. The superplasticizer (SP) and water were subsequently added, and mixing proceeded until a homogenous consistency was attained (Fig. 4b). The fresh concrete was immediately put to the required fresh properties tests (slump flow, T500, L-box and sieve segregation). Following completion of these tests, the concrete was cast into the designated moulds (Fig. 4c) and demoulded 24 hours later for water curing (Fig. 5a and 5b).

Table 2. Mix design for HFC incorporating 0-20% ESP as a partial replacement for OPC

Mixture ID	OPC (kg/m³)	ESP (%)	ESP (kg/m³)	Coarse Aggregate (kg/m³)	Fine Aggregate (kg/m³)	Water (litre/ m³)	Super plasticizer (litre/kg/m³)
C100	480	NA	0	760	890	215	9.6
C95-ESP5	456	5	24	760	890	215	9.6
C90-ESP10	432	10	48	760	890	215	9.6
C85-ESP15	408	15	72	760	890	215	9.6
C80-ESP20	384	20	96	760	890	215	9.6

**Note: C95-ESP5:*

C: Cement

95: 95% of OPC

ESP: Eggshell Powder

5: 5% of ESP

(a)

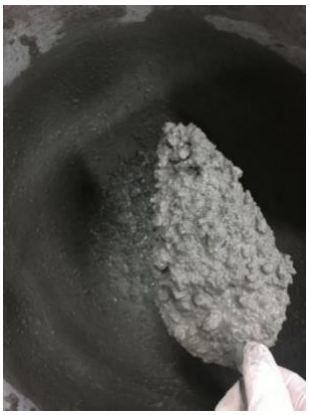

(b)

(c)

Fig. 4. Mixing and casting process for HFC: (a) addition and blending of materials in the mixer; (b) homogeneous HFC mix; (c) freshly cast HFC specimens in moulds

(a)

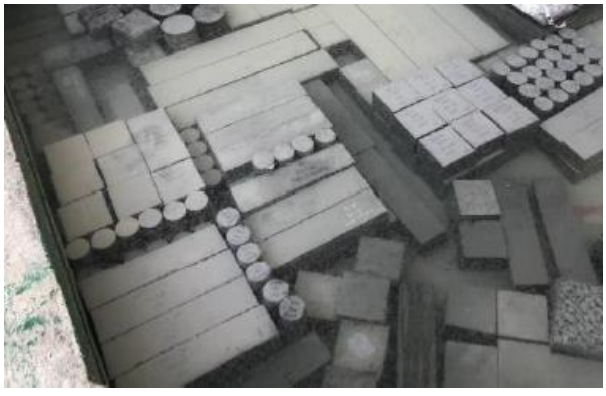

(b)

Fig. 5. HFC specimens: (a) after demoulding at 24 hours; (b) undergoing water curing.

All mixing, casting, curing, and testing were performed under controlled laboratory conditions (23 ± 2 °C and 60-70% relative humidity). These controlled environmental settings assured that the fresh and hardened performance of the HFC mixtures was primarily determined by material composition rather than external changes, thus improving the experimental results' reliability and uniformity. Besides that, to make sure methodological consistency and traceability, every phase of experimentation adhered entirely to internationally recognized standards, BS EN 12350 for fresh properties [14, 15, 16], BS EN 12390-3 for compressive strength [17], and ASTM C496 for splitting tensile strength [18], which aligning the testing procedure with worldwide concrete evaluation practices. In addition, each mechanical properties test was carried out on three replicate specimens per mix, and all values provided include the mean and standard deviation to demonstrate statistical confidence and repeatability.

Based on this validated testing framework, the current study's experimental scope was specifically restricted to first-phase essential assessments in order to gain a controlled comprehension of ESP's direct influence on early-age rheology and strength advancement. Other characterization methods such as U-box flow assessment, V-funnel viscosity assessment, flexural strength, UPV, water absorption, and durability indicators are designed for a subsequent extended study as part of the HFC-ESP system evaluation.

2.2. Fresh Properties of the HFC Mixtures

The fresh properties of HFC, specifically flowability, passing ability, and segregation resistance, were assessed in compliance with the EFNARC guidelines using the standardized approaches outlined in [14], [15], and [16].

2.2.1 Slump Flow and T500 Test

Flowability and flow rate were assessed using the slump flow test and T_{500} measurement as stated in BS EN 12350-8:2010 [14]. The slump flow test assesses HFC's ability to spread under its own weight, whereas T_{500} examines the time needed for the spread to achieve a 500 mm diameter in the presence of obstacles. The set-up had a 900 × 900 mm base plate and a typical slump cone, as shown in Fig. 6. After mixing, the clean cone was placed in the center of the base plate and filled with fresh concrete. Any spills were cleared prior to testing. The cone was then raised vertically, and the stopwatch was started when it lost touch with the base plate. The T_{500} time was recorded once the concrete spread reached a diameter of 500 mm. The final slump flow diameter was measured in two perpendicular directions (d_1 and d_2), and the average value was estimated as given in Equation (1).

$$D = \frac{d_1 + d_2}{2} \tag{1}$$

(a) (b)

Fig. 6. Equipment and measurement procedure for the slump flow and T500 test: (a) Experiment set-up; (b) diameter measurement (d_1 and d_2)

2.2.2 L-Box test

The L-Box test, as specified in BS EN 12350-10:2010 [15], was used to determine passing ability. This approach analyzes HFC's ability to flow into restricted spaces such as reinforcement gaps, without segregation. The apparatus is L-shaped, with a vertical part (inlet) coupled to a horizontal section that simulates restricted flow (Fig. 7). Fresh HFC was introduced into the vertical part, and the gate was lowered to enable free flow under gravity (Fig. 8a). Concrete heights were calculated at the end of the horizontal segment (H_2) and vertical part (H_1) (Figs. 8b and 8c). The passing ability (PA) was evaluated using Equation (2) as follows:

$$PA = \frac{H_2}{H_1} \tag{2}$$

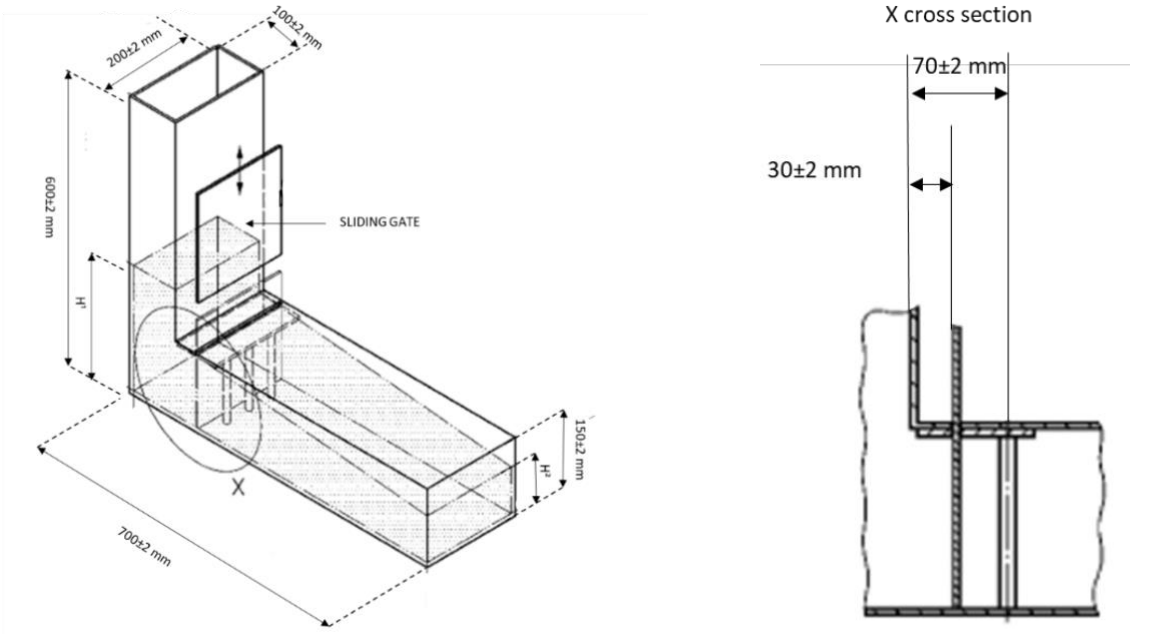

(a) (b)

Fig. 7. Illustration of the L-Box test: (a) full dimensions and equipment used, (b) cross-section of the L-Box. [15]

(a) (b) (c)

Fig. 8. L-Box test: (a) full view of the L-Box; (b) H_1 measurement; (c) H_2 measurement

2.2.3 Sieve Segregation Test

Segregation resistance was measured in line with BS EN 12350-11:2010 [16], used to examine the resistance of HFC to segregation. The initial mass of fresh concrete (m_c) was measured before it was placed on a 5 mm sieve over a sieve receiver (Fig. 9). After two minutes, the sieve was carefully removed upwards, and the combined mass of the receiver and passing material (m_{ps}) was measured. The mass of the sieve receiver (m_p) was also recorded. The segregation ratio (SR) was computed as given in Equation (3):

$$SR = \frac{(m_{ps} - m_p)\, x\, 100}{m_c} \quad (3)$$

(a) (b) (c)

Fig. 9. Sieve segregation test: (a) experimental set-up [16]; (b) fresh concrete poured onto the sieve; (c) weighing the mass of the sieve receiver with the passed concrete

2.3. Hardened Properties of The HFC Specimens

Compressive and split tensile strength tests were performed to assess the hardened properties of HFC. The compressive strength test was carried out in line with [17], a basic approach for measuring the ultimate load capacity and structural integrity of concrete samples, as shown in Fig. 10. Under compression test, this study utilized 100 mm × 100 mm cube specimens that were water-cured for 7, 28 and 90 days. Testing was conducted using a 1000 kN compression testing equipment, which applied an axial compressive load until the specimen failed. The optimal blend was chosen by considering the highest compressive strength obtained from all HFC specimens.

(a) (b)

Fig. 10. Experimental setup of HFC specimens under compressive loading and split tensile strength: (a) cubic specimen; (b) cylindrical specimen

Meanwhile, the split tensile strength test was carried out in line with [18] to determine the concrete's tensile resistance. Cylindrical specimens with dimensions of 100 mm in height and 50 mm in diameter were produced and water-cured for 7, 28 and 90 days. Each specimen was placed horizontally between two loading platens, and a compressive force was exerted across its vertical diameter until failure occurred. This generated tensile strains in the specimen's cross-section, causing it to break. The splitting tensile strength (T_s) was estimated as shown in Equation (4) after calculating the maximum load at failure.

$$T_s = \frac{2P}{\pi DL} \tag{4}$$

In which, T_s denotes the splitting tensile strength in kPa, P embodies the maximum applied load indicated by the testing machine in kN, D as diameter of the sample and L represents the length of the specimen in m.

3. Results and Discussion

Considering that additional fresh, hardened, microstructure and durability-related tests such as U-box, and V-funnel, flexural capacity, SEM, EDX, UPV, sorptivity and chloride penetration, are needed for a more in-depth structural evaluation, the present findings are a crucial initial phase in offering a foundational understanding of ESP's influence on the flowability, viscosity, stability, and mechanical behavior of HFC. Identifying this baseline performance requires attention before proceeding to more extensive performance-based assessments. In line with this aim, the current study conducts a systematic investigation into the fresh properties of HFC mixes, the hardened properties of the resulting specimens, the correlation between compressive and splitting tensile strengths in comparison to previous studies, and the typical modes of failure. All of these aspects are further explained in detail within the subsequent sub-sections.

3.1. Fresh Properties of The HFC Mixes

Table 3 exhibits the experimental findings for highly flowable concrete (HFC) rheological properties tests such as slump flow, T500, L-Box, and sieve segregation.

Table 3. Results of the rheological properties of HFC containing ESP

Sample	Slump flow (mm)	T500 (sec)	L-Box, PA	Sieve Segregation, SR%
C100	626	7	0.90	10.22
C95-ESP5	610	8	0.89	8.82
C90-ESP10	580	11	0.83	6.74
C85-ESP15	563	13	0.81	5.28
C80-ESP20	680	6	0.42	15.21
EFNARC, 2005 [19]	550-650 (SF1) 660-750 (SF2) 760-850 (SF3)	<2 (VS1) ≥ 2 (VS2)	≥ 0.80 with 2 rebars (PA1) ≥ 0.80 with 3 rebars (PA2)	≤ 20 (SR1) ≤ 15 (SR2)

Table 3 depicts the five investigated mixtures (C100, C95-ESP5, C90-ESP10, C85-ESP15, and C80-ESP20), with four of them (C100, C95-ESP5, C90-ESP10, and C85-ESP15) falling into the SF1 category based on the [19] (slump flow). C80-ESP20, on the other hand, is classified as SF2 since its slump flow value falls between 660 and 750 mm. These categories relate to diverse uses, with SF1 being advised for unreinforced or minimally reinforced slabs cast from the top, and SF2 better suited for vertical structural elements that include walls and columns. Fig. 11 shows a minor decline in flowability with an increase in ESP substitution up to 15%, followed by a significant improvement when 20% ESP was added. The comparable T500 measurements (Fig. 12) reveal that at 20% ESP, the slump flow time increased significantly from 7 to 13 s before decreasing to 6 s. This trend indicates the influence of ESP on the rheological behavior of the SCC, where gradual replacement in the range of 5-15% results in increasing viscosity, but over this threshold (20%)

the mix exhibits increased fluidity. These experimental findings are consistent with previous studies [11,20,21,22], which have consistently shown that the inclusion of ESP modifies the workability of HFC, resulting in comparable flow characteristics. The agreement across various tests supports the evidence that ESP is a promising supplementary material for HFC manufacturing, with flow performance suitable for a wide range of structural applications.

The addition of ESP to the HFC mix has a considerable influence on segregation resistance, as shown by the sieve segregation outcomes (Fig. 13). Segregation was reduced when ESP content increased up to 15%, but segregation resistance fell substantially at 20% replacement. EFNARC classifications divide segregation ratios (SR) into two categories, which are SR1 and SR2. Fig. 13 demonstrates that mixes C100, C95-ESP5, C90-ESP10, and C85-ESP15 fall under the SR2 classification. This classification is deemed appropriate for vertical elements with flow distances higher than 5 m and confinement gaps greater than 80 mm, in which increased segregation resistance is necessary to ensure homogeneity throughout placement. Meanwhile, C80-ESP20 has been designated as SR1, suitable for thin slabs and vertical uses with lower flow distances (< 5 m) and comparable confinement circumstances. These categories emphasize the significance of properly choosing ESP content to balance flowability and segregation resistance in various structural applications. Increasing ESP amounts by up to 15% enables improved resistance to segregation, improving the reliability and quality of SCC in challenging placement situations. [23] published similar findings, showing that mixes containing 5%, 10%, and 15% ESP consistently attained SR2 categorization.

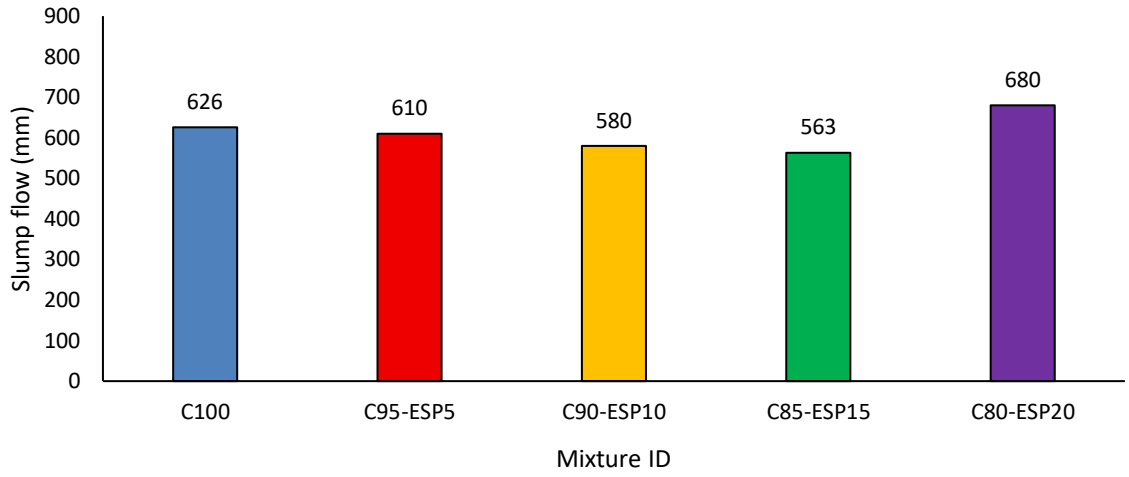

Fig. 11. Slump flow experimental results of HFC mixes

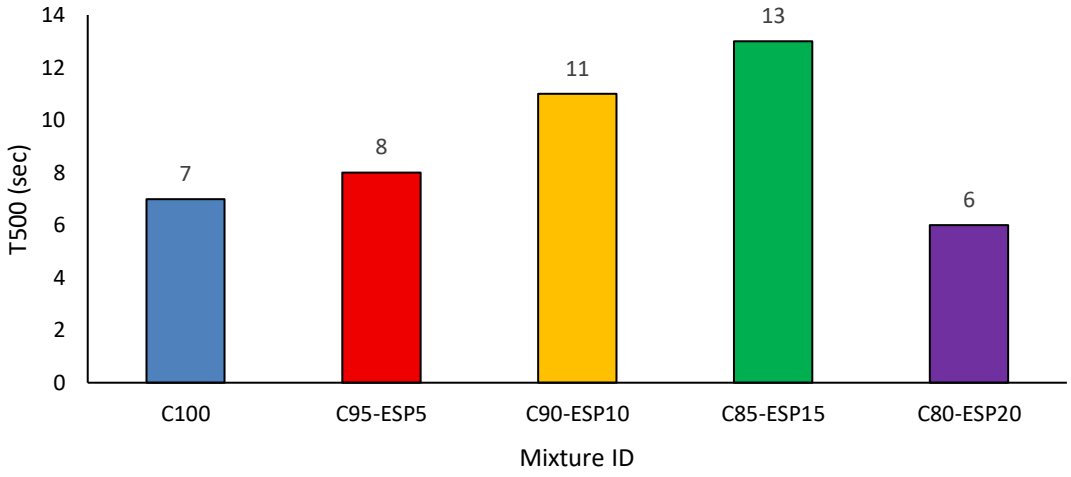

Fig. 12. T500 experimental results of HFC mixes

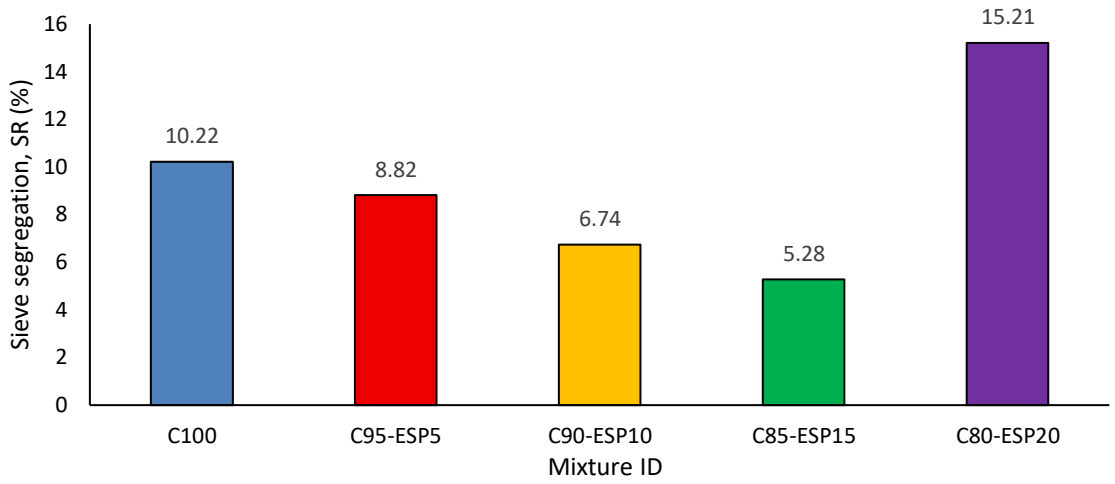

Fig. 13. Sieve segregation test results of HFC mixes incorporating varying ESP contents

The study's results indicates that partial ESP substitution improves segregation resistance in HFC, especially for vertical applications with longer flow distances and wider confinement gaps. In addition, these findings provide strong evidence that ESP is a feasible supplemental material to generate HFC with improved segregation control in a variety of practical settings.

On the other hand, Fig. 14 shows a gradual decrease in the passing ability (PA) ratio as ESP replacement increases in 5% increments. The PA ratio decreased from 0.90 to 0.42, demonstrating that the ability of HFC mixtures to flow through confined spaces becomes increasingly constrained as ESP level increases. All mixes were evaluated with three reinforcing bars as obstacles. Despite only the mix of C80-ESP20, all mixes' PA ratios remained over 0.80, meeting the PA2 categorization based on EFNARC criteria. This classification indicates mixes suited for complicated structural elements with reinforcing gaps of less than 60 mm. However, it should be noted that full-scale mock-up tests might need to be performed to verify what was found under actual construction settings.

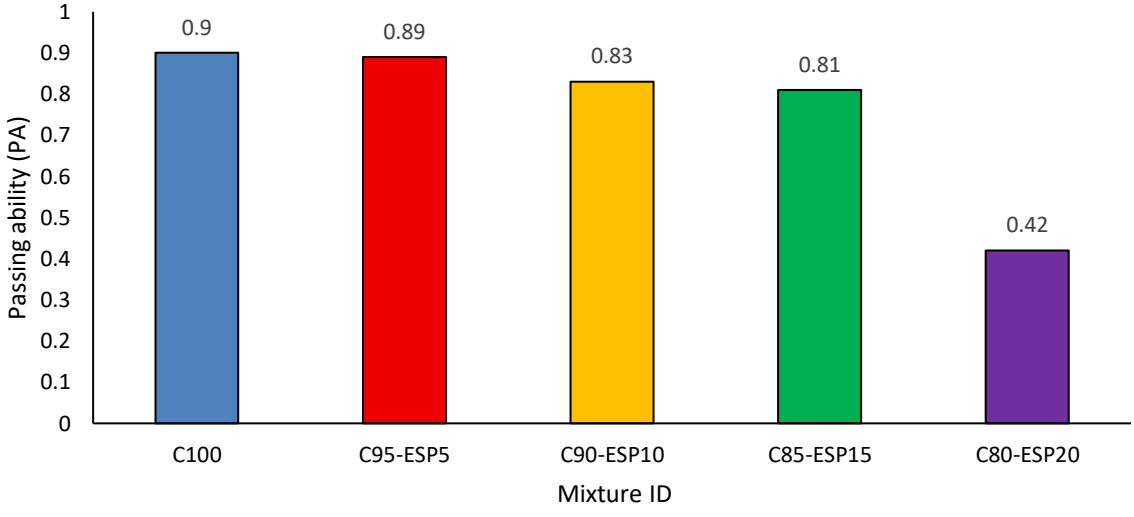

Fig. 14. L-box (passing ability) test results of HFC mixes incorporating varying ESP

The trend seen in this study (Fig. 14) is consistent with earlier research. [7], [11] and [22] all reported similar results, with HFC blends encompassing ESP showing PA2 classification with decreasing PA ratios. Additionally, [24] found a deviation to this general pattern, emphasizing the potential impact of combination proportions and testing conditions on passing ability outcomes. The observed decrease in PA ratio with increasing ESP concentration demonstrates the sensitivity of HFC rheology to fine supplementary materials. Greater ESP replacement limits the mix's ability

to handle congested reinforcement zones, which affects flowability and passing performance. Thus, the results obtained give compelling evidence that maximizing ESP concentration is critical for balancing flow and passage properties in highly flowable concrete, ensuring its use in complicated reinforced structural systems.

3.2. Hardened Properties of The HFC Specimens

All HFC specimens were loaded progressively until failure occurred. Table 4 displays the compression test results for the HFC specimens, with average values calculated from the three specimens. The strength progression pattern presented in Table 4 clearly indicates the effect of ESP concentration on HFC behavior at both early age and long term. At 7 days, the control mix (C100) had an average compressive strength of 29.23 MPa, whereas adding ESP at 5%, 10%, and 15% resulted in increases of 33.83 MPa, 45.90 MPa, and 46.47 MPa, respectively. The substantial improvement at 10-15% replacement suggests that finely ground ESP's micro-filler effect enhanced particle packing and reduced internal voids, promoting early hydration and matrix densification. Nevertheless, at 20% replacement (C80-ESP20), the 7-day compressive strength dropped to 38.93 MPa, implying that excessive cement dilution starts to outweigh its beneficial filler effect.

Table 4. Comparative compressive strength (CS) test results of HFC specimens (7 and 28 days)

Mix ID	7 days			28 days			90 days		
	CS (N/mm^2)	Mean (N/mm^2)	STD	CS (N/mm^2)	Mean (N/mm^2)	STD	CS (N/mm^2)	Mean (N/mm^2)	STD
C100	27.66 29.89 30.13	29.23	1.36	37.88 39.16 39.51	38.85	0.86	80.13 75.76 77.35	77.75	2.212
C95-ESP5	32.90 34.38 34.22	33.83	0.81	48.44 49.05 51.16	49.55	1.43	55.65 55.19 51.39	54.08	2.338
C90-ESP10	45.03 46.16 46.51	45.90	0.77	53.54 56.21 56.84	55.53	1.75	47.11 50.98 51.16	49.75	2.288
C85-ESP15	44.48 45.78 49.16	46.47	2.42	56.41 59.86 59.13	58.47	1.82	38.74 45.81 46.18	43.58	4.193
C80-ESP20	39.29 41.02 36.48	38.93	2.29	49.52 50.64 48.96	49.71	0.86	42.54 47.07 42.19	43.93	2.722

A comparable pattern of compressive strength can also be seen after 28 days. The control mix attained 38.85 MPa, while C95-ESP5, C90-ESP10, and C85-ESP15 recorded 49.55, 55.53, and 58.47 MPa, respectively. The maximum strength performance at 15% ESP demonstrates that, at modest replacement levels, ESP improves microstructural compactness and load transfer efficiency inside the hardened HFC matrix. The decrease in the amount at 20% ESP (49.71 MPa) contributes support to the concept that beyond an optimal threshold, clinker content dilution restricts the creation of primary hydration products (C-S-H), thus lowering the progression of strength.

The 90-day findings offer a better understanding of long-term hydration behavior and matrix stability. The control mix's strength increased significantly to 77.75 MPa, demonstrating that cement particles hydrated continuously throughout time. Additionally, the 90-day strength of HFC specimens incorporating 5% and 10% ESP (54.08 MPa and 49.75 MPa, respectively) did not exceed the control, and higher replacement levels resulted in a significant reduction (43.58 MPa for 15% and 43.93 MPa for 20%). This behavior indicates that, while ESP improves early- and medium-age strength through physical densification, its contribution to long-term strength is primarily due to the filler effect rather than a strong pozzolanic reaction. ESP is primarily $CaCO_3$-based, compared

to supplementary cementitious ingredients like GGBS or silica-rich pozzolans, which increase long-term strength via secondary C-S-H production. As a result, its long-term contribution is mostly dependent on microstructural refinement and nucleation effects, instead of ongoing chemical response. Higher replacement levels (≥15%) cause more dilution over time, resulting in less clinker available for hydration and lower 90-day strengths.

The results of these studies suggest that the ideal ESP replacement level for balancing early-age enhancement and long-term performance is between 10-15%. At this level, enhanced particle packing and ITZ refinement allow for partial cement reduction without affecting long-term hydration potential. Yet, substitute levels exceeding 15% could adversely impact long-term hardened performance owing to inadequate cementitious binder concentration. These findings emphasize ESP's potential as a supplementary cementitious material to improve the mechanical properties of HFC. Previous studies by [7,11,20, 21,22,23] and [25] have all reported consistent results, particularly in terms of strength development at early (7-day) and standard (28-day) curing periods.

The presence of 90-day data from this study thus offers an extensive understanding of ESP-modified HFC behavior, demonstrating that ESP acts mainly as a micro-filler and hydration accelerator instead of a highly reactive pozzolan. The subsequent research will extend curing times to 56 days and beyond 90 days and add durability assessments (e.g., permeability, sorptivity, and microstructural analysis) in order to further clarify long-term performance mechanisms.

On the other hand, the consistently low standard deviations (STD) recorded for all mixtures show that the compressive strength data are resilient, indicating a good level of experimental precision and reproducibility. Furthermore, the strength growth of the ESP-modified mixtures is consistent with established behaviour patterns for SCC with CaO-dominant additional materials, as recorded in earlier research [10,11,23]. The congruence of the current findings with a wider body of literature offers external validation and strengthens confidence in the reliability of the observed mechanical benefits at moderate ESP substitute levels.

The split tensile strength (STS) test yields similar findings as compressive strength. This correlation was anticipated considering both tests utilize a similar type of concrete. The split tensile strength in Table 5 was computed using the empirical formula, which is given by Equation 4.

Table 5. Results of the split tensile strength of HFC

Mix	7 days			28 days			90 days		
	STS, F_{st} (N/mm²)	Mean (N/mm²)	STD	STS, F_{st} (N/mm²)	Mean (N/mm²)	STD	STS, F_{st} (N/mm²)	Mean (N/mm²)	STD
C100	2.44 2.50 2.64	2.53	0.10	3.09 3.16 3.20	3.15	0.06	4.38 4.56 4.00	4.31	0.29
C95-ESP5	2.75 2.84 2.97	2.85	0.11	3.55 3.72 3.81	3.69	0.13	2.25 2.55 3.14	2.65	0.45
C90-ESP10	3.03 3.09 3.11	3.08	0.04	3.74 3.99 4.18	3.97	0.22	3.49 3.22 3.87	3.53	0.33
C85-ESP15	3.48 3.65 3.81	3.65	0.17	3.82 4.15 4.23	4.07	0.22	3.31 3.22 3.41	3.31	0.10
C80-ESP20	3.11 3.22 2.65	2.99	0.30	3.96 3.71 3.37	3.68	0.30	3.19 4.31 3.37	3.62	0.60

Table 5 demonstrates the splitting tensile strength findings for the concrete specimens at various curing ages, offering information on their long-term mechanical characteristics. In general, all HFC

specimens containing ESP showed an enhancement in splitting tensile strength after 7 days of curing in contrast to the control mix (C100). C85-ESP15 had the maximum strength (3.65 MPa), followed by C90-ESP10 (3.08 MPa), and C95-ESP5 had the lowest (2.85 MPa). At 28 days, the performance trend was consistent. C85-ESP15 also had the highest splitting tensile strength (4.07 MPa), followed by C90-ESP10 (3.97 MPa). In contrast, C80-ESP20 and C95-ESP5 had substantially lower strengths of 3.68 MPa and 3.69 MPa. These results show that ESP addition had a substantial effect on the splitting tensile strength of the concrete specimens.

The increase in splitting-tensile strength can also be attributed to ESP's micro-filler effect, which refines pore structure, increases matrix cohesion, and leads to a more uniform stress distribution under splitting-tensile loading. The greater CaO concentration in ESP may potentially induce secondary hydration products within the ITZ, increasing the relationship between paste and aggregates which contributes to the higher splitting-tensile strengths measured at moderate ESP amounts. Comparisons across specimens illustrate that moderate ESP amounts, such as 10-15%, improve splitting tensile strength, typically exceeding the control mix and low ESP replacement (C95-ESP5). However, the results drop noticed in C95-ESP5 after 28 days implies that excessively reduced ESP inclusion may not be beneficial to tensile strength growth. Meanwhile, higher ESP amounts, such as 20%, led to a decline in strength, suggesting the presence of an optimal substitution threshold.

The 90-day findings reveal additional details about the long-term split-tensile performance of the ESP-modified HFC. The strength of the control mix (C100) increased steadily to 4.31 MPa, indicating continuous cement hydration and matrix densification. For HFC specimens, C90-ESP10 (3.53 MPa) and C80-ESP20 (3.62 MPa) exhibited comparable split-tensile strength at 90 days, while C85-ESP15 recorded a slight reduction to 3.31 MPa. Meanwhile, C95-ESP5 demonstrated a more noticeable decrease (2.65 MPa), indicating that lower ESP content may not be sufficient to sustain long-term tensile enhancement. The measured 90-day performance shows that, whereas ESP successfully improves early and intermediate split-tensile strength via micro-filler densification and increased ITZ cohesion, its long-term contribution is limited by cement availability and hydration continuity. As a result, at greater substitution levels, cement dilution diminishes long-term hydration products, potentially slowing split-tensile strength development when compared to the control mix. Nonetheless, the 10-15% replacement range exhibits rather steady long-term tensile performance, demonstrating that ESP integration does not degrade structural tensile resistance when utilized within an appropriate range.

In general, the findings show that adding ESP boosted splitting tensile strength up to an optimum level, beyond which its effectiveness gradually decreased. The observed trend highlights the occurrence of an optimal ESP range for maximizing tensile strength, which is consistent with earlier findings in compressive strength development. Furthermore, the correlation between compressive strength and splitting tensile strength was found to be similar across specimens, with higher compressive strength often resulting in higher splitting tensile strength. This correlation highlights the synergistic effect of ESP incorporation on the hardened performance of concrete specimens.

3.3. Experimental Observations and Literature-Based Comparisons on The Strength Correlation in HFC Specimens

There was a significant relationship between compressive strength and splitting tensile strength in the investigated HFC specimens. In order to estimate splitting tensile strength from compressive strength, numerous empirical equations formulated by previous studies were investigated and compared to the experimental findings gathered during this study. The inclusion of the splitting tensile test serves as crucial to ensuring a more thorough evaluation of the mechanical properties of HFC with ESP as a partial substitute for cement. Furthermore, using well-established prediction correlations from previous studies, the splitting tensile strength can be estimated without the need for significant laboratory testing.

In this study, a power-type relationship has been proposed using regression analysis to assess the correlation among compressive and splitting tensile strengths. Fig. 15 indicates that the splitting tensile strength increased proportionally with the compressive strength for all HFC

specimens incorporating ESP. Based on this relationship, a prediction model was developed and expressed as Equation (6), which resulted from regression analysis of the experimental results gained after 28 days of curing.

$$. F_t = 0.3095 f_{ck}{}^{0.6343} \quad (6)$$

In which, F_t denotes the split tensile strength and f_{ck} signifies the compressive strength of HFC specimens.

Fig. 15 exhibits a significant correlation (R^2 = 0.9987) between compressive and splitting tensile strengths, supporting the proposed power-type regression model. Table 6 summarizes the estimated splitting tensile strength values obtained from this regression equation, as well as the comparison results from previous studies.

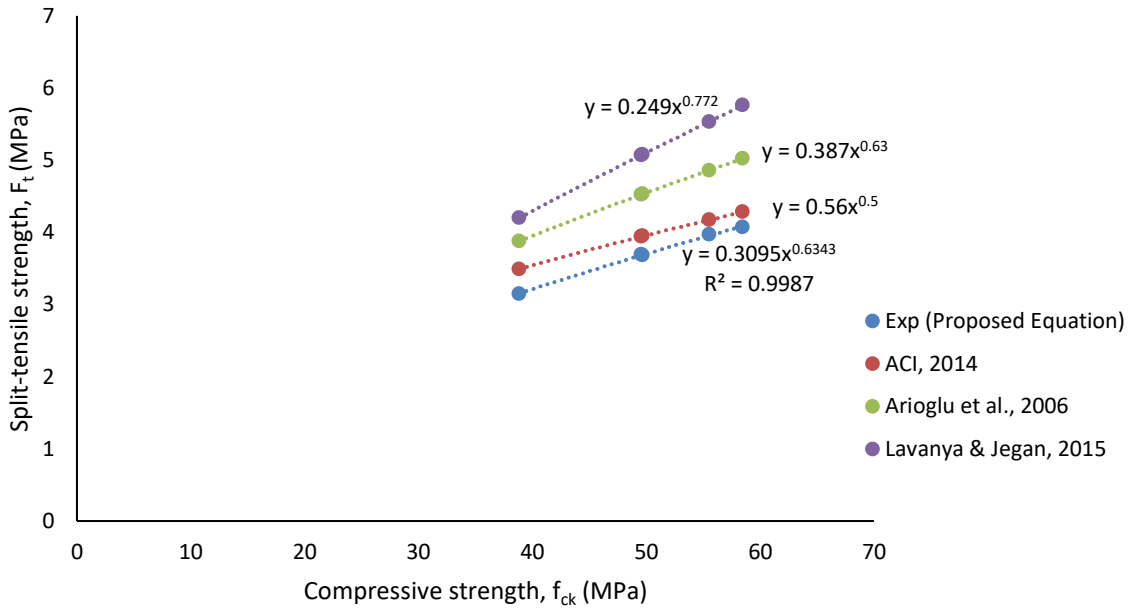

Fig. 15. Correlation between splitting tensile and compressive strengths of HFC incorporating ESP after 28 days of water curing

Table 6. Comparison of splitting tensile strength of hardened HFC specimens with previous studies

Mix	Compressive strength (MPa) (28 days), f_{ck}	Split tensile strength (MPa) (28 days), f_t	Proposed Equation $F_t = 0.3095 f_{ck}{}^{0.6343}$ (Equation 6)	[26] $F = 0.56 f_{ck}{}^{0.5}$	[25] $F = 0.387 f_{ck}{}^{0.63}$	[22] $F = 0.249 f_{ck}{}^{0.772}$
C100	38.85	3.15	3.15	3.49	3.88	4.20
C95-ESP5	49.55	3.69	3.68	3.94	4.52	5.067
C90-ESP10	55.53	3.97	3.96	4.17	4.86	5.53
C85-ESP15	58.47	4.07	4.09	4.28	5.02	5.76
C80-ESP20	49.71	3.68	3.69	3.95	4.53	5.08

The comparison of the results in Table 6 reveals that the proposed regression equation has the best agreement with the experimental splitting tensile strength values for all specimens. As an instance,

in the C95-ESP5 and C90-ESP10 specimens, the estimated strengths from the proposed model (3.68 MPa and 3.96 MPa, respectively) are almost identical to the experimental data (3.69 MPa and 3.97 MPa). In contrast, the [26] equation continually provides somewhat higher values, with discrepancies ranging from 5 to 10%. Even though the difference is small, it implies that the ACI model, which was designed largely for conventional concretes, does not fully represent the effect of ESP on the tensile behavior of HFC. Prediction drawn from [25] exhibit higher variations, overestimating splitting tensile strength by 20% or more, as seen in the C90-ESP10 specimen, where the model gives 4.86 MPa versus the experimental 3.97 MPa. Even bigger splitting tensile values are observed with the equation of [22], which provides the highest predicted values among all models. For instance, the C85-ESP15 specimen has a predicted value of 5.76 MPa compared to the experimental 4.07 MPa, reflecting a discrepancy of over 40%. These disparities demonstrate that empirical data derived from conventional or alternative concrete systems may not be immediately applicable to ESP-modified HFC.

Besides that, to assess the predictive accuracy of Equation (6), the 28-day experimental dataset was employed for calculating statistical indicators such as coefficient of determination (R^2), mean absolute error (MAE), and root mean square error (RMSE). The proposed model had a R^2 value of 0.999, with MAE and RMSE values of 0.010 and 0.012 MPa, respectively, suggesting a strong correlation between projected and experimental splitting tensile strength values. For comparison, previously developed empirical models produced substantially greater prediction errors. Model [26] produced R^2 = 0.35 with MAE = 0.254 MPa and RMSE = 0.259 MPa. Models [25] had significantly bigger deviations with MAE = 0.846 MPa and RMSE = 0.865 MPa. While model [22] with MAE = 1.411 MPa and RMSE = 1.428 MPa. These models typically overestimated splitting tensile strength, implying a limited applicability to non-calcined ESP-modified HFC. Equation (6) performs well because it was calibrated using experimental data relevant to the examined material system, capturing the effect of ESP-induced microstructural densification on tensile behaviour.

This study emphasizes the fundamental relationship of compressive and splitting tensile strengths and shows an effective predictive method for calculating splitting tensile strength from compressive strength of HFC encompassing ESP. The regression model developed in this study provides a useful tool for both the development and the performance assessment of ESP-based concrete. However, additional experimental validation under various mix proportions, curing settings, and material compositions would be beneficial to verify the proposed model's strength and practicality. However, despite its good predictive capability in the examined range, the model that was suggested is empirical and relies on a small dataset (ESP replacement 0-20%). Extrapolation beyond the given range or usage to calcined ESP systems, different binder compositions, or various conditions of curing needs to be done with caution. The model also does not adequately take into consideration microstructural features including porosity evolution, hydration degree, and ITZ properties, all of which might have an impact on splitting tensile performance. In order to enhance generalizability, additional experimental validation under various mix proportions, curing settings, and material compositions would be beneficial to verify the proposed model's strength and practicality.

3.4. Mode of Failure

In the present study, cracking patterns resulting from compressive and splitting-tensile strength tests were systematically examined, as shown in Fig. 16 and Fig. 17. Concrete fails in different ways based on the type of loading and stress conditions used. These modes are primarily driven by fracture formation and propagation inside the cementitious matrix and at the aggregate-paste contact. A better understanding of this overall failure mechanism lays the basis for the following explanation of the various fracture mechanisms that are discovered under compressive and splitting-tensile loads.

(a) (b) (c) (d) (e)

Fig. 16. Cracking patterns of HFC specimens under compressive loading: (a) C100 (control), (b) C95-ESP5, (c) C90-ESP10, (d) C85-ESP15, and (e) C80-ESP20

Fig. 16 (a-e) and Table 7 depict the cracking patterns of 100 × 100 mm HFC specimens under compressive loading. The control specimen (C100) showed substantial and critical vertical cracking, implying a brittle fracture mode, as depicted in Fig. 16(a). Vertical edge cracks were also observed in specimens containing 5% and 10% ESP (C95-ESP5 and C90-ESP10). However, their initiation points varied, where C95-ESP5 showed cracking along the lower left edge, whereas C90-ESP10 showed cracks at the upper left side, as can be seen in Fig. 16(b-c). On the contrary, specimens containing greater ESP replacement levels (C85-ESP15 and C80-ESP20) exhibited only small surface fractures, with C80-ESP20 having the least apparent damage (Fig. 16(d-e)). Overall, the severity and amount of cracking decreased as ESP content increased. The addition of ESP reduces crack propagation in HFC by densifying the matrix and lowering stress concentrations. Nonetheless, the overall cracking pattern was consistent with that of control specimen (C100), which is characterized by vertical fracture formation under compressive stress.

Table 7. Type of crack recorded on HFC cube specimens under compressive loading

Specimen designation	Type of cracks	
	Vertical	Edge
C100	Yes	Yes
C95-ESP5	Yes	Yes
C90-ESP10	Yes	Yes
C85-ESP15	Yes	Yes
C80-ESP20	Yes	Yes

(a) (b) (c) (d) (e)

Fig. 17. Cracking patterns of HFC specimens under splitting tensile strength test: (a) C100 (control), (b) C95-ESP5, (c) C90-ESP10, (d) C85-ESP15, and (e) C80-ESP20

Table 8. Crack patterns observed in cylindrical specimens subjected to the splitting tensile strength test

Specimen designation	Type of cracks
	Vertical
C100	Yes
C95-ESP5	Yes
C90-ESP10	Yes
C85-ESP15	Yes
C80-ESP20	Yes

Fig. 17(a-e) and Table 8 exhibit the pattern of cracks of 50 × 100 mm cylindrical specimens subjected to the splitting tensile test for various HFC specimens. Different crack formation patterns were detected based on the ESP content (5%, 10%, 15% and 20%). The control specimen (C100), showed a noticeable and continuous crack pattern, indicating a typical brittle tensile failure, as depicted in Fig. 17(a). In contrast, C95-ESP5 exhibited more severe cracking, showing a decrease in tensile resistance with reduced ESP incorporation (Fig. 17(b)). In addition, cracks in C90-ESP10 were mostly found throughout the middle part of the specimen, indicating a more localized failure pattern, as shown in Fig. 17(c). Remarkably, the specimen with the highest ESP concentration (C80-ESP20) exhibited the least obvious cracking, with cracks reaching only to approximately two-thirds of the specimen's height, as can be seen in Fig. 17(e). C85-ESP15 showed much more cracking than C80-ESP20, which indicates that larger ESP replacement levels could lead to enhanced crack resistance via the micro-filler effect and increased matrix densification, as observed in Fig. 17(d).

The crack patterns that were noticed are comparable with the compression test results (Fig. 16), which demonstrated that the use of ESP reduced the severity of cracking. This shows that ESP improves HFC tensile performance by refining pore structure, reducing stress concentrations, and delaying crack propagation. [27] also discovered that partial ESP substitution improves cementitious materials' mechanical properties by serving as a micro-filler and densifying the matrix. Furthermore, several studies show that utilizing up to 20% ESP can increase concrete strength and durability by refining the pore structure and lowering stress concentrations [28]. However, more research is needed to understand the underlying mechanisms at the microstructural level and to determine the ideal ESP content for maximum tensile strength as well as durability in practical applications.

4. Conclusions

This study carefully explored the potential utilization of ESP as a partial cement substitution in HFC. The results demonstrate that ESP has a considerable impact on both the fresh and hardened properties of HFC, highlighting its ability to serve as a sustainable alternative binder. In accordance with the experimental findings and analysis, several significant conclusions can be drawn concerning the use of eggshell powder (ESP) as a supplementary cementitious material in highly flowable concrete (HFC):

- Increased ESP content resulted in variations in fresh properties such as slump flow diameter and T500 time. A significant increase in flowability was observed with 20% ESP substitution. According to EFNARC classification, the resulting SF1 and SF2 classifications show that HFC incorporating ESP can be adapted for a variety of structural applications, covering unreinforced or moderately reinforced parts to widespread structural use.
- For segregation resistance, ESP generally reduced sieve segregation, with the exception of 20% replacement, where segregation increased significantly. The calculated segregation ratio (SR) values attributed to the SR1 and SR2 categories, providing practical recommendations on permitted flow distances and confinement gaps.
- The addition of eggshell powder (ESP) greatly improved the hardened properties of HFC after 7, 28, and 90 days. Compressive strength (CS) increased significantly with 10-15% substitution, especially at early and intermediate ages, owing to better particle packing and microstructural densification. Even though the control mix exhibited the highest 90-day strength, ESP-modified mixes in the optimum range exhibited steady and structurally sufficient performance over the long term.
- Splitting tensile strength (STS) showed a similar trend, with 10-15% ESP improving fracture resistance and paste-aggregate bonding after 7 and 28 days. STS remained steady after 90 days, with no indication of long-term deterioration. ESP functions largely as a micro-filler and nucleation agent, with a 10-15% substitute level suggested to maximize strength development while maintaining long-term mechanical strength. To accurately measure long-term strength evolution and durability properties, extended curing times (56 and beyond 90 days) could be employed in the subsequent phase of this study.

- The addition of ESP in HFC enhances crack propagation resistance under both compressive and tensile loading, with higher ESP replacement levels (particularly 15-20%) enhancing the micro-filler effect and matrix densification, which leads to lesser crack severity and more localized or less noticeable failure patterns in contrast to the brittle and continuous cracks found in the control specimen.

Therefore, incorporating ESP with HFC provides considerable benefits in terms of sustainability and usage. ESP minimizes the consumption of cement and CO_2 emissions while promoting waste recycling, consistent with sustainable construction and circular economy concepts. While the present investigation shows that ESP improves the fresh and hardened characteristics of HFC, the results are mostly focused on early-age performance. In order to enhance ESP's usability as a sustainable cement substitute, future study should look into long-term durability in harsh conditions, microstructural behaviors, and optimal adjustment of ESP particle size and percentages of substitution. Even though a thorough techno-economic analysis was not within the scope of the present investigation, preliminary findings indicate that substituting 10-15% of cement with non-calcined ESP may lower binder-related material costs, given that cement accounts for a significant amount of concrete production prices. The reduction of calcination lowers processing energy requirements and operational costs. Furthermore, valorizing industrial eggshell waste could decrease disposal costs and promote sustainable economic practices. Future research should include life-cycle cost analysis (LCCA) and large-scale feasibility studies to quantify economic and environmental advantages, contribution to low-carbon and sustainable construction methods. Recognizing these needs, the study also recognized that further investigations, such as flexural behaviour, ultrasonic pulse velocity (UPV), absorption properties, flow assessments including the U-box and V-funnel and long-term durability tests like microstructure, shrinkage, chloride ingress, and carbonation, could enhance the overall understanding of HFC incorporating ESP. These concerns will be tackled in a forthcoming supplementary study as part of the second phase of this research effort.

Acknowledgement

The authors acknowledge the technical assistance provided by the staff of the Concrete, Fabrication, and Heavy Structures Laboratories, Faculty of Civil Engineering, Universiti Teknologi MARA (UiTM), Shah Alam.

References

[1] Goyal A. Comparison of self-compacting concrete (SCC) containing fly ash and ground granulated blast furnace slag. International Journal of Engineering Research and Science, 2017;3(4):27-34.
[2] Scrivener KL, John VM, Gartner EM. Eco-efficient cements: Potential economically viable solutions for a low-CO_2 cement-based materials industry. Cement and Concrete Research, 2018;114:2-26. https://doi.org/10.1016/j.cemconres.2018.03.015
[3] Our World in Data. CO_2 emissions in Malaysia. Our World in Data, 2024.
[4] Rasiah S, Farrokhzadi F, Lahoud A. Properties of flowing concrete and self-compacting concrete with high-performance superplasticizer. Proceedings of the 3rd International RILEM Symposium, Reykjavik, Iceland, 2003:1048.
[5] Leelavathi R, Sudalaimani K. Study on self-compacting concrete with GGBS and M-sand. Polish Journal of Environmental Studies, 2021;30(6):1-12. https://doi.org/10.15244/pjoes/135827
[6] Elbasri OMM, Sghaiar S, Shubaili M, Abdullah GMS, Abdullah MZ. Performance of self-compacting concrete incorporating wastepaper sludge ash and pulverized fuel ash as partial substitutes. Case Studies in Construction Materials, 2022;17:e01459. https://doi.org/10.1016/j.cscm.2022.e01459
[7] Mahesh S. Self compacting concrete and its properties. Journal of Engineering Research and Applications, 2014;4:72-80.
[8] Djeddou M, Amieur M, Chaid R, Mesbah HA. Development of eco-friendly self-compacting concrete using marble powder, blast furnace slag and glass fibre-reinforced plastic waste: Application of mixture design approach. Research on Engineering Structures and Materials, 2025;11(1):113-138. http://dx.doi.org/10.17515/resm2024.178ma0208rs
[9] Rebai B, Benaddi H, Messas T, Salhi M. Evaluation of self-compacting concrete for concrete repair applications. Research on Engineering Structures and Materials, 2025;11(2):495-513. http://dx.doi.org/10.17515/resm2024.255st0423rs
[10] Tan YY. Eggshell as a partial cement replacement in concrete development. Magazine of Concrete Research, 2017;70(13):662-670. https://doi.org/10.1680/jmacr.17.00003

[11] Jhatial AA, Sohu S, Memon MJ, Bhatti N. Eggshell powder as partial cement replacement and its effect on the workability and compressive strength of concrete. International Journal of Advanced and Applied Sciences, 2019;6(9):71-75. https://doi.org/10.21833/ijaas.2019.09.011
[12] Krishta T, Rosdee NAM, Sivaraos, Sivakumar S. Self-compacting concrete containing fly ash, silica fume and rice husk ash. AIP Conference Proceedings, 2024;3161(1):020108. https://doi.org/10.1063/5.0229816
[13] Muhammad A, Thienel KC. Properties of self-compacting concrete produced with optimized volumes of calcined clay and rice husk ash: Emphasis on rheology, flowability retention and durability. Materials, 2023;16(16):5513. https://doi.org/10.3390/ma16165513
[14] British Standards Institution. Testing fresh concrete - Part 8: Self-compacting concrete - Slump-flow test. BS EN 12350-8, Brussels, 2010.
[15] British Standards Institution. Testing fresh concrete - Part 10: Self-compacting concrete - L-box test. BS EN 12350-10, Brussels, 2010.
[16] British Standards Institution. Testing fresh concrete - Part 11: Self-compacting concrete - Sieve segregation test. BS EN 12350-11, Brussels, 2010.
[17] British Standards Institution. Testing hardened concrete - Part 3: Compressive strength of test specimens. BS EN 12390-3, 2009.
[18] American Society for Testing and Materials. Standard test method for splitting tensile strength of cylindrical concrete specimens. ASTM C496/C496M-04, ASTM International, 2004.
[19] EFNARC. The European guidelines for self-compacting concrete: Specification, production and use. EFNARC, 2005.
[20] Hamdullah DN, Hama SM, Yaseen MM. Effect of eggshell waste powder on impact resistance and bond characteristics of reinforced concrete. Key Engineering Materials, 2020;870:21-28. https://doi.org/10.4028/www.scientific.net/KEM.870.21
[21] Hilal N, Al Saffar DM, Ali TKM. Effect of eggshell ash and strap plastic waste on properties of high strength sustainable self-compacting concrete. Arabian Journal of Geosciences, 2021;14:4. https://doi.org/10.1007/s12517-021-06654-x
[22] Lavanya G, Jegan J. Evaluation of relationship between split tensile strength and compressive strength for geopolymer concrete of varying grades and molarity. International Journal of Applied Engineering Research, 2015;10:35523–35529.
[23] Md Zain MR, Oh CL, Lee SW. Investigations on rheological and mechanical properties of self-compacting concrete containing 0.6 μm eggshell as partial replacement of cement. Construction and Building Materials, 2021;303:124539. https://doi.org/10.1016/j.conbuildmat.2021.124539
[24] Ofuyatan OM, Adeniyi AG, Ijie D, Ighalo JO, Oluwafemi J. Development of high-performance self compacting concrete using eggshell powder and blast furnace slag as partial cement replacement. Construction and Building Materials, 2020;256:119403. https://doi.org/10.1016/j.conbuildmat.2020.119403
[25] Arıoğlu N, Girgin ZC, Arıoğlu E. Evaluation of ratio between splitting tensile strength and compressive strength for concretes up to 120 MPa and its application in strength criterion. ACI Materials Journal, 2006;103(1):18–24. https://doi.org/10.14359/15123
[26] American Concrete Institute. Building code requirements for structural concrete (ACI 318-14). American Concrete Institute, 2014.
[27] Sathiparan N. Utilization prospects of eggshell powder in sustainable construction material – A review. Construction and Building Materials, 2021;293:123465. https://doi.org/10.1016/j.conbuildmat.2021.123465
[28] Paruthi S, Khan AH, Kumar A, et al. Sustainable cement replacement using waste eggshells: A review on mechanical properties of eggshell concrete and strength prediction using artificial neural network. Case Studies in Construction Materials, 2023;18:e02160. https://doi.org/10.1016/j.cscm.2023.e02160